18
Channels and pipes

Even the most common of fluid flows, the water coming out of the kitchen tap or the draught of air around you, are so full of little eddies that it seems totally beyond exact analysis. Fluid mechanics is the story of coarse approximation, gross oversimplification, and if everything else fails and results are required, numeric computation.

Analytic solutions of the Navier-Stokes equations are few and hard to come by, even for steady flow. They are always found in geometries characterized by a high degree of symmetry, for example planar, cylindrical or spherical. Then again, even if the geometry of a problem — the containing boundaries — are perfectly symmetric, there is no guarantee that the analytic solutions obeying these symmetries are the ones that the actual fluid selects as its flow pattern.

Symmetry is only a guideline. There may and will in any geometry be flows that are not maximally symmetric. At low Reynolds number one expects that the maximally symmetric solution might be stable against disturbances, but at large Reynolds number this will not be the case. The simple laminar flow pattern of the maximally symmetric steady flow is then broken, spontaneously or by little irregularities in the geometry, and replaced by turbulent time-dependent motion with less than maximal symmetry, or no symmetry at all.

In this chapter we shall study steady laminar flow in the simplest of geometries: planar and cylindrical. The exact solutions presented here are all effectively one-dimensional and thus lead to ordinary differential equations that are easy to solve. Although the solutions are all of infinite extent they nevertheless provide valuable insight into the behavior of viscous fluids for moderate Reynolds number. For completeness we also describe the phenomenology of turbulent pipe flow, secondary flow and Taylor vortices. In appendix 19 the numerical solution to laminar channel entrance flow is computed.

18.1 Steady, incompressible flow

It has been remarked before that most of the fluids in our daily life, water, air, gasoline, and oil, are effectively incompressible as long as flow velocities are well below the speed of sound. In looking for exact solutions we shall assume that the density is everywhere constant $\rho(\boldsymbol{x}, t) = \rho_0$ such that the divergence condition,

$$\boxed{\mathsf{div}\, \boldsymbol{v} = 0} \,, \tag{18-1}$$

is always satisfied. Dividing the Navier-Stokes equation (17-12) with ρ_0 and setting $\partial \boldsymbol{v}/\partial t = \boldsymbol{0}$ we obtain the basic equation for steady, incompressible flow

$$\boxed{(\boldsymbol{v} \cdot \boldsymbol{\nabla})\boldsymbol{v} = -\frac{1}{\rho_0}\boldsymbol{\nabla} p + \nu \boldsymbol{\nabla}^2 \boldsymbol{v} + \boldsymbol{g}} \,, \tag{18-2}$$

where ν is the kinematic viscosity (17-6). In principle, these four partial differential equations for the four fields, v_x, v_y, v_z and p, determine the fields everywhere inside a control volume, when provided with suitable boundary conditions that fix the values of the fields or their derivatives on the surface of the volume. In practice, however, we often solve these equations by making assumptions about the form of the fields, based on the symmetries of the particular problem at hand.

Symmetry assumptions always limit the possible boundary conditions that may be imposed on the fields. In the absence of gravity, the field equations are, for example, always solved by the extremely "symmetric" solution, $\boldsymbol{v} = \boldsymbol{0}$ and $p = 0$, but this assumption will indeed prevent us from selecting any non-zero values for the fields or their derivatives on the boundaries. Symmetry assumptions always make the solution blind to the symmetry breakdown that may happen in the real world of turbulent fluids. So, it should never be forgotten, that although symmetric solutions can be beautiful, they may in fact also be wrong!

Effective pressure

The gravitational field $\boldsymbol{g} = -\boldsymbol{\nabla}\Phi$ on the right hand side of (18-2) can in fact be absorbed in the pressure gradient. If we define the *effective* or *piezometric* pressure,

$$p^* = p + \rho_0 \Phi \,, \tag{18-3}$$

gravity may formally be removed from (18-2), and we obtain the even simpler field equation for the velocity field,

$$(\boldsymbol{v} \cdot \boldsymbol{\nabla})\boldsymbol{v} = -\frac{1}{\rho_0}\boldsymbol{\nabla} p^* + \nu \boldsymbol{\nabla}^2 \boldsymbol{v} \,. \tag{18-4}$$

The effective pressure is constant in the hydrostatic case as can be seen by setting $\boldsymbol{v} = \boldsymbol{0}$, and represents in general the *extra* pressure necessary to sustain the flow. It should however be kept in mind that it is the true pressure p and not p^* which appears in Stokes' stress tensor (17-10).

18.2 Planar geometry

Planar flow may, for example, be realized by enclosing fluid between parallel plates. In section 17.1 we discussed the special case, where one of the plates was moving at constant velocity with respect to the other. In a coordinate system with the y-axis orthogonal to the plates, we assume as before that the velocity field is of the form

$$\boldsymbol{v} = (v_x(y), 0, 0) = v_x(y)\, \boldsymbol{e}_x \ . \qquad (18\text{-}5)$$

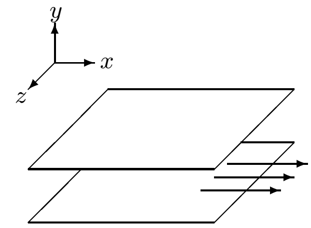

Planar flow between parallel plates.

An infinitely extended flow like this is of course unphysical, but the ideal planar solution should nevertheless offer an approximation to the real flow between plates of finite extent, provided the dimensions of the plates are sufficiently large compared to their distance.

General solution

With the assumed form of the flow, the incompressibility condition (18-1) is automatically fulfilled, $\mathsf{div}\, \boldsymbol{v} = \nabla_x v_x(y) = 0$. The inertial acceleration vanishes likewise, $(\boldsymbol{v} \cdot \boldsymbol{\nabla})\boldsymbol{v} = v_x(y)\nabla_x(v_x(y), 0, 0) = \boldsymbol{0}$. Intuitively, both of these conclusions follow from the flow lines all being parallel, neither diverging or converging, nor changing direction. The Navier-Stokes equation for incompressible fluid (18-4) now expresses that the (effective) pressure gradient everywhere has to balance the viscous drag,

$$\boldsymbol{\nabla} p^* = \eta\ \boldsymbol{e}_x \boldsymbol{\nabla}^2 v_x(y)$$

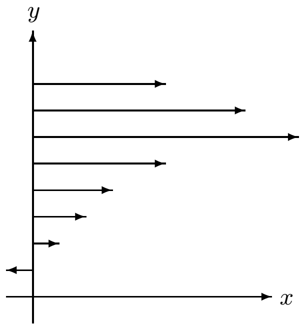

A possible planar flow profile.

From the y and z components of this equation we get $\nabla_y p^* = \nabla_z p^* = 0$, implying that the effective pressure cannot depend on y and z, or in other words $p^* = p^*(x)$. The x-component of the equation takes the form,

$$\frac{dp^*(x)}{dx} = \eta \frac{d^2 v_x(y)}{dy^2} \ .$$

The left hand side depends only on x and the right hand side only on y. This is only possible, if both sides take the same value independently of both x and y. Denoting the common value $-G$ we find immediately the solution for the effective pressure

$$\boxed{p^* = p_0 - Gx} \ , \qquad (18\text{-}6)$$

where p_0 is a constant. For $G > 0$, the effective pressure falls linearly with increasing x and this is intuitively consistent with the fluid being driven in the positive x-direction by pressure or gravitational forces.

The velocity field is finally found by solving the second order differential equation $\eta\, d^2 v_x/dy^2 = -G$, and becomes

$$\boxed{v_x(y) = -\frac{G}{2\eta} y^2 + Ay + B} \ , \qquad (18\text{-}7)$$

where A and B are integration constants. This is the most general form of the planar velocity field consistent with the fundamental equations (18-1) and (18-4), and thus with Newtonian mechanics. The only freedom left in the planar flow problem lies in the two integration constants, and they will be fixed by the boundary conditions to be applied in specific situations to be discussed in the following two sections.

18.3 Pressure driven flow between fixed plates

Suppose that a channel is defined by two infinitely extended static plates, one at $y = 0$ and the other at $y = d$. Such a flow can be approximately realized by forcing fluid under pressure in between large parallel plates of size $L_x \times L_z$ with $L_{x,z} \gg d$. If the pressure drop is Δp between the entry at $x = 0$ and the exit at $x = L_x$, the pressure gradient becomes $G = \Delta p/L_x$.

Alternatively, one can make the parallel plates vertical with the x-axis pointing downwards and let gravity alone drive the flow. In that case the effective pressure gradient is given by the gravitational field, $G = -\nabla_x p^* = -\rho_0 \nabla_x \Phi = \rho_0 g_0$, but otherwise the problem (and the solution) is the same. If the plates are inclined an angle α to the horizontal, the effective pressure gradient is instead $G = \rho_0 g_0 \sin\alpha$.

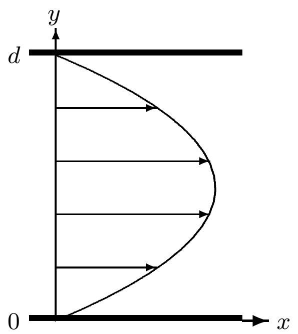

Characteristic parabolic velocity profile between the plates, driven by a pressure which is higher to the left than to the right.

Applying the no-slip boundary conditions, $v_x(0) = v_x(d) = 0$, we obtain $A = Gd/2\eta$ and $B = 0$, so that the velocity field becomes,

$$\boxed{v_x(y) = \frac{G}{2\eta} y(d-y)} \ . \qquad (18\text{-}8)$$

It has a characteristic parabolic shape with the largest velocity $Gd^2/8\eta$ in the middle of the gap, $y = d/2$.

Discharge rate and average velocity

The total volume fluid passing between the plates per unit of time, also called the *volumetric discharge rate*, is obtained by integrating the velocity field over the area $d \times L_z$ between the plates,

$$Q = \int_0^d v_x(y)\, L_z dy = \frac{G L_z d^3}{12\eta} \ . \qquad (18\text{-}9)$$

From the discharge rate we may calculate the average velocity of the flow in the gap

$$U = \frac{1}{d}\int_0^d v_x(y)\, dy = \frac{Q}{L_z d} = \frac{Gd^2}{12\eta} \ . \qquad (18\text{-}10)$$

It grows quadratically with the distance between the plates, but intuitively this is not so surprising, because with increasing distance the friction from the walls becomes less and less important. In the extreme limit of infinite distance, it takes of course no pressure gradient to maintain a flow with a given velocity U everywhere.

Reynolds number

The Reynolds number (17-14) has been defined as the ratio between convective and viscous terms in the Navier-Stokes equation. But we have seen that in planar flow the inertial acceleration always vanishes, so the Reynolds number must strictly speaking be zero. How can that be?

The apparent paradox is resolved when we consider what happens when the driving pressure gradient grows larger. Laminar flow is then replaced by irregular, time-dependent, turbulent flow with non-vanishing convective contributions. The Reynolds number should be understood as a dimensionless characterization of the ratio of convective to viscous forces in terms of the speed and geometry of the general flow. For planar flow the Reynolds number may therefore always be taken to be

$$\mathsf{Re} = \frac{Ud}{\nu} , \tag{18-11}$$

where U is the average flow velocity and d is the thickness of the fluid layer.

One may rightly wonder why one uses the plate distance rather than the size of the plates in calculating the Reynolds number. The answer is that the character of the flow is primarily determined by the interplay between the friction from the plates and the inertia of the fluid, whereas cross-stream and downstream the plates act uniformly on the fluid and no new phenomena come into play.

In the laminar case the average velocity U is directly proportional to the pressure gradient G, as shown by (18-10). When the flow turns turbulent at a Reynolds number of the order of 2000, the relation between average velocity and pressure gradient becomes non-linear, and the laminar formalism is no more correct. The phenomenology of turbulent pressure driven planar flow is quite similar to that of turbulent pressure driven pipe flow which is presented in section 18.7 on page 313.

Example 18.3.1: Let oil ($\eta = 2 \times 10^{-2}$ Pa s and $\rho_0 = 800$ kg/m^3) be forced between plates that are $d = 1$ cm apart by a pressure gradient of 10^3 Pa/m. The average velocity becomes in this case $U \approx 0.4$ m/s corresponding to a Reynolds number of $\mathsf{Re} \approx 167$. The discharge rate per unit of length orthogonal to the flow $Q/L_z \approx 4$ liter/s/m.

If the plates were instead placed vertically, the pressure gradient would be $G = \rho_0 g_0 \approx 8000$ Pa/m, leading to $U \approx 3.3$ m/s, $\mathsf{Re} \approx 1333$ and $Q/L_z \approx 33$ liter/s/m.

18.4 Gravity driven flow with an open surface

Before refrigeration became commonplace, food shops would sometimes have a thin water "curtain" flowing down the inside of store-front windows as a cooling

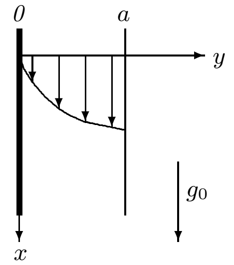

Vertical gravity driven flow with an open surface. The velocity profile is half of the velocity profile between vertical parallel fixed plates.

device, in cheese shops also used to reduce smell. The water was fed in on top of the window and driven down the window by gravity alone. The water sheet was reasonably stable as long as it remained thin, although the shimmering look that one got through the window pane indicated that it might not be far from instability.

Let us assume that the water sheet has constant thickness a. On the window surface, $y = 0$, the no-slip condition again demands $v_x(0) = 0$, leading to $B = 0$. If we disregard the interaction with the air (see problem 18.4), there will be no forces acting on the open water surface at $y = a$. This implies that the shear stress must vanish, *i.e.* $dv_x/dy = 0$ for $y = a$, leading to $A = \rho_0 g_0 a/\eta$. With $G = \rho_0 g_0$, the solution therefore becomes

$$\boxed{v_x(y) = \frac{g_0}{2\nu} y(2a - y)} , \tag{18-12}$$

where ν is the kinematic viscosity (17-6). In this case, the dynamic viscosity has completely disappeared, leaving only the kinematic viscosity, as it should when the flow is characterized by kinematic parameters only, here g_0.

The profile is parabolic as before, but now has its maximum at the open surface. In retrospect we could have derived it from the flow between fixed plates by setting $d = 2a$, because the shear stress in that case vanishes in the middle $y = a$ between the plates. The open surface velocity profile is simply half of the velocity profile between fixed plates. The average velocity may either be obtained by integrating the velocity field or by putting $d = 2a$ in (18-10)

$$U = \frac{1}{a} \int_0^a v_x(y)\, dy = \frac{g_0 a^2}{3\nu} . \tag{18-13}$$

The total discharge rate for a window of horizontal length L becomes

$$\boxed{Q = ULa = \frac{g_0 L a^3}{3\nu}} , \tag{18-14}$$

which is (of course) half of the discharge rate between parallel plates at distance $d = 2a$. In practice, one would probably solve this equation for a,

$$a = \left(\frac{3\nu}{g_0}\frac{Q}{L}\right)^{\frac{1}{3}} , \tag{18-15}$$

and thus determine the thickness of the layer from the amount of fluid, Q/L, fed into the window per unit of horizontal length.

Example 18.4.1: Feeding water in at a rate of $Q/L = 100\ \mathsf{cm^3/s/m}$ of a storefront window leads to a sheet thickness $a = 0.3$ mm and a velocity of $U \approx 34$ cm/s, corresponding to Re ≈ 230, well below the onset of turbulence.

18.5 Tubular geometry

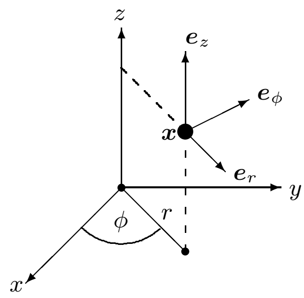

Cylindrical coordinates and basis vectors.

An infinitely long circular cylindrical tube is invariant both under translations along its axis and rotations around it. We shall in this section only be interested in longitudinal flow along the axis of the tube. In a coordinate system with the z-axis running along the cylinder axis, we therefore assume the following form for the velocity field,

$$\boldsymbol{v} = (0, 0, v_z(r)) = v_z(r)\boldsymbol{e}_z \ , \tag{18-16}$$

where $r = \sqrt{x^2 + y^2}$ is the radial distance from the cylinder axis (see section 2.7). This field is evidently invariant under translations along the cylinder axis as well as rotations around it, and is therefore maximally symmetric with respect to the cylindrical geometry. In section 18.9, we consider another maximally symmetric flow which circles around the cylinder axis.

General solution

As in the planar case, the flow lines are all parallel, implying that the assumed field (18-16) must be free of divergence, $\mathsf{div}\,\boldsymbol{v} = \nabla_z(v_z(r)\boldsymbol{e}_z) = 0$. Similarly, the inertial acceleration also vanishes for the same reason; formally because $\boldsymbol{v}\cdot\boldsymbol{\nabla}\boldsymbol{v} = v_z(r)\,\nabla_z(v_z(r)\boldsymbol{e}_z) = \boldsymbol{0}$. The Navier-Stokes equation (18-2) simplifies to,

$$\boldsymbol{\nabla} p^* = \eta\ \boldsymbol{e}_z \boldsymbol{\nabla}^2 v_z(r) \ , \tag{18-17}$$

where p^* is the effective pressure (18-3). From the x and y-components of this equation we get $\nabla_x p^* = \nabla_y p^* = 0$, and consequently the pressure can only depend on z, *i.e.* $p = p(z)$. The Laplacian on the right hand side is given by (2-60) but may also be found by straightforward calculation (see also problem 18.8),

$$\begin{aligned}
\boldsymbol{\nabla}^2 v_z(r) &= \left(\frac{\partial^2}{\partial x^2} + \frac{\partial^2}{\partial y^2}\right) v_z(r) = \left(\frac{\partial}{\partial x}\frac{x}{r} + \frac{\partial}{\partial y}\frac{y}{r}\right)\frac{dv_z(r)}{dr} \\
&= \frac{2}{r}\frac{dv_z(r)}{dr} + (x^2 + y^2)\frac{d}{dr}\left(\frac{1}{r}\frac{dv_z(r)}{dr}\right) \\
&= \frac{1}{r}\frac{dv_z(r)}{dr} + \frac{d^2 v_z(r)}{dr^2} \ .
\end{aligned}$$

Rewriting the last expression, the z-component of (18-17) becomes,

$$\frac{dp^*(z)}{dz} = \eta \frac{1}{r}\frac{d}{dr}\left(r\frac{dv_z(r)}{dr}\right) \ . \tag{18-18}$$

The left hand side of this equation depends only on z whereas the right hand side depends only on r, so neither side can depend on r and z. Denoting the common constant value by $-G$, we obtain as for planar flow

$$\boxed{p^*(z) = p_0 - Gz} \ , \tag{18-19}$$

where p_0 is an integration constant. The most general solution to the velocity field is obtained by setting the righthand part of (18-18) equal to $-G$ is,

$$\boxed{v_z(r) = -\frac{G}{4\eta}r^2 + A\log r + B}\,, \tag{18-20}$$

with two integration constants, A and B.

18.6 Laminar pipe flow

Jean-Louis-Marie Poiseuille (1799–1869). *French physician who studied blood circulation and performed experiments on flow in tubes. Presumably the first to have measured blood pressure by means of a mercury manometer.*

Gotthilf Heinrich Ludwig Hagen (1797–1884). *German hydraulic engineer, specialized in waterworks, harbors and dikes.*

Cylindrical pipes carrying effectively incompressible fluids are ubiquitous, in industry, in the home, and in our own bodies. Household water and almost all other fluids are transported under pressure in long pipes with circular cross sections. The question of how much fluid a given pressure can drive through a circular tube is one of the most basic problems in fluid mechanics and was first addressed quantitatively by Poiseuille around 1841 (and unbeknownst to the physics community at that time, independently by Hagen in 1839)[1]. Today *Poiseuille flow* is often used to denote any pressure driven laminar flow, for example also the planar flow between fixed plates discussed on page 304.

Poiseuille velocity field

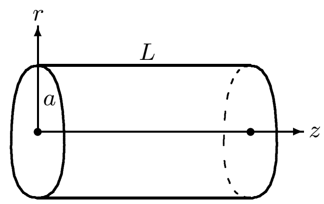

Section of a circular pipe of inner radius a and length L. There is a pressure drop Δp between $z = 0$ and $z = L$ which drives the flow of fluid through the pipe.

Let a stretch of pipe have (inner) radius a and length L, and let the flow be driven by a pressure drop $\Delta p = p(0) - p(L)$ between the ends of the pipe (and no gravity). We assume that this section of pipe is cut out of a much longer pipe, so that there will be no special circumstances to account for at the ends. When the fluid runs in the positive z-direction the pressure must be higher at the entry, say at $z = 0$, than at the exit, $z = L$, so that the negative of the pressure gradient along the z-axis, $G = \Delta p/L$, is positive.

The fluid velocity cannot be infinite at $r = 0$, and consequently we must have $A = 0$ in the general solution (18-20). The no-slip boundary condition requires that $v_z(a) = 0$, and this fixes the last integration constant to $B = Ga^2/4\eta$, so that the longitudinal velocity profile becomes

$$\boxed{v_z(r) = \frac{G}{4\eta}(a^2 - r^2)}\,. \tag{18-21}$$

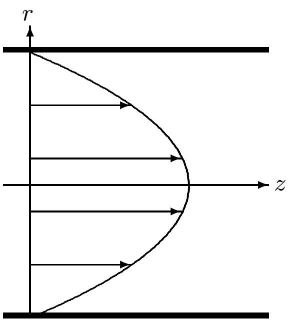

Velocity profile for laminar flow through a circular pipe.

It is parabolic as for planar flow and reaches, as one would expect, its maximal value $U_{\max} = Ga^2/4\eta$ at the center of the pipe. Incidentally, this formula was

[1]There is some confusion in the literature on the precise years. The original references are: G. H. L. Hagen, *Über die Bevwegung des Wassers in engen cylindrischen Rohren*, Poggendorfs Annalen der Physik und Chemie **16** (1839) and J. L. Poiseuile, *Recherches experimentales sur le mouvement des liquides dans les tubes de tres petits diametres*, Compte-rendus hebdomadaire des Seances de l'Academie des Sciences (1841).

not derived theoretically by Poiseuille in the way we have done here but rather by Hagenbach and Neumann around 1859. What an entangled web we physicists weave.

The Hagen-Poiseuille law

The volumetric discharge rate, *i.e.* the volume of fluid carried through the pipe per unit of time, may immediately be calculated by integrating the velocity field over the cross section of the pipe,

$$\boxed{Q \equiv \int_0^a v_z(r)\, 2\pi r\, dr = \frac{\pi G a^4}{8\eta}} \ . \tag{18-22}$$

This is the famous *Hagen-Poiseuille law.* As could have been expected, the throughput grows linearly with the pressure gradient, and inversely with viscosity. The dramatic fourth power growth with radius could of course have been deduced from dimensional arguments since it is the only missing factor. The growth expresses as in the planar case that the friction from the walls becomes less and less important in holding back the fluid as the radius grows.

Reynolds number

The velocity of the flow averaged over the cross section of the pipe may be calculated from the rate of discharge,

$$U = \frac{Q}{\pi a^2} = \frac{G a^2}{8\eta} \ . \tag{18-23}$$

It is exactly half the maximal velocity found at the center of the pipe. As for planar flow, there is a formal problem in defining the Reynolds number, because the convective term vanishes, but as we discussed there the Reynolds number may nevertheless be defined to be,

$$\mathsf{Re} = \frac{2aU}{\nu} = \frac{\rho_0 G a^3}{4\eta^2} \ . \tag{18-24}$$

The choice of the pipe diameter $d = 2a$ as length scale and not the radius is purely a matter of convention. Reynolds himself actually used the radius [35, p. 85].

Pipe flow remains laminar until turbulence sets in at a Reynolds number somewhere between 2000 and 4000, typically 2300 for smooth pipes. At that point the otherwise linear relationship between volume discharge and pressure gradient becomes non-linear. The phenomenology of turbulent pipe flow will be discussed in section 18.7.

Example 18.6.1 (Aortic flow): Human blood is not a particularly Newtonian fluid, but approximatively its viscosity may be taken to be $\eta = 4 \times 10^{-3}$ Pa s and its density near that of water. The blood flow rate in the aorta (averaged over a heartbeat) is about $Q \approx 70$ cm^3/s. Since the diameter of the aorta is $2a \approx 35$ mm the average velocity becomes $U \approx 70$ cm/s and the Reynolds number Re ≈ 600, well below the turbulent region. The pressure gradient becomes $G \approx 7$ Pa/m, showing that the pressure drop is negligible in the large arteries compared to blood pressure, $p \approx 15,000$ Pa.

Example 18.6.2 (Water pipe): Household water supply has to reach the highest floor in apartment buildings with pressure "to spare". Pressures must therefore be of the order of bars when water is not tapped. The typical discharge rate from a kitchen faucet is around $Q \approx 100$ cm^3/s, leading to an average velocity in a half-inch pipe of about $U \approx 0.8$ m/s. The Reynolds number is about Re $\approx 11,600$ which is well inside the turbulent regime. The pressure gradient calculated from the Hagen-Poiseuille law, $G \approx 140$ Pa/m, is for this reason untrustworthy.

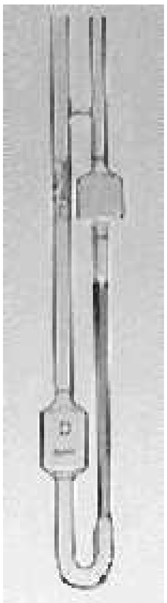

Commercial Ostwald viscometer (produced by Poulten Selfe & Lee, Great Britain). One measures the time it takes the liquid surface to pass between the marks on the container on the right (on its way to the container on the left through the capillary pipe section) and compares it with the corresponding time for a calibration liquid of known viscosity.

Wilhelm Ostwald (1853–1932). *German scientist, considered the father of modern physical chemistry. Invented the Ostwald process for synthesizing nitrates still used in manufacture of explosives. Received the Nobel prize in chemistry in 1909.*

Ostwald viscometer

The Hagen-Poiseuille law (18-22) may be used experimentally to determine the viscosity of a fluid from a measurement of the pressure drop $\Delta p = GL$ and the total volume $V = QT$ of fluid discharged from the pipe in the time interval T. The simplest way to create a precisely defined effective pressure drop is to place the pipe vertically in the gravitational field, such that the effective pressure gradient becomes $G = \rho_0 g_0$. Inserting this into (18-22) we find the kinematic viscosity

$$\boxed{\nu = \frac{\eta}{\rho_0} = \frac{\pi a^4 G}{8\rho_0 Q} = \frac{\pi a^4 g_0 T}{8V}} \ . \tag{18-25}$$

The *Ostwald viscometer* is entirely made from glass with no moving parts, and one obtains the kinematic viscosity of a liquid by measuring the passage time for a known volume of liquid through a narrow section of pipe. We shall later calculate the terminal velocity for the laminar draining of viscous liquid through a pipe (section 18.8).

The viscosity determined in this way is only meaningful for laminar flow which requires the Reynolds number to be smaller than about 2000. From (18-24) we obtain the Reynolds number for the viscometer,

$$\mathrm{Re} = \frac{g_0 a^3}{4\nu^2} \ . \tag{18-26}$$

and this shows that for water-like liquids with $\nu \approx 10^{-6}$ m^2/s the tube radius must be smaller than 1 mm in order to avoid turbulence, *i.e.* it must be a capillary tube.

Pipe resistance

The pressure drop, $\Delta p = GL$, necessary to drive a given volume flux Q through a section of a pipe is completely analogous to the voltage drop necessary to drive an electric current through a conducting wire. In analogy with Ohm's law, the quantity

$$R = \frac{\Delta p}{Q} = \frac{8\eta L}{\pi a^4} \ , \tag{18-27}$$

may be called *pipe resistance*. It depends only on the viscosity of the fluid and the dimensions of the pipe and is measured in the strange unit $\mathsf{kgm^{-4}s^{-1}}$. Like electric resistance, pipe resistance is additive for pipes connected in series and reciprocally additive for pipes connected in parallel (see problem 18.11).

Friction

The flow through the pipe is steady so that the amount of momentum is constant in the fixed control volume consisting of all the fluid in the pipe section of length L. Since the fluid enters and leaves the pipe at the same velocity, the rate of loss of momentum from the control volume is zero, which in turn implies that the total force on the volume must vanish. The component of the total force in the direction of the flow consists of the force $\pi a^2 \Delta p$ due to the difference in pressure between the ends of the control volume, plus the friction force (or drag) $-\mathcal{D}$ exerted on the fluid by the walls of the pipe. The drag is made explicitly negative because viscosity acts as a brake on the flow. Equating the total force to zero, $\pi a^2 \Delta p - \mathcal{D} = 0$, we get

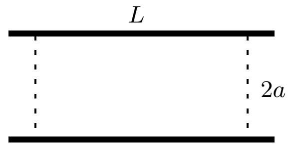

The static control volume of length L.

$$\mathcal{D} = \pi a^2 \Delta p = \pi a^2 L G = 8\pi\eta U L \ . \tag{18-28}$$

Here the Poiseuille expression (18-23) has been used to express the drag in terms of the average velocity. The linear growth of drag with velocity is characteristic of laminar fluid flow. In turbulent flow non-linearity sets in.

The friction is caused by the shear stress on the fluid in contact with the wall of the pipe,

$$\sigma_{zr} = \eta \nabla_r v_z(r)\big|_{r=a} = -\frac{1}{2} G a \ . \tag{18-29}$$

Multiplying with the inner area of the pipe $2\pi a L$ we obtain again the expression for the drag $\sigma_{zr} 2\pi a L = -\pi a^2 L G$, as we ought to.

Is the drag small or large? There seems no way of comparing it with anything else since the only other force acting on the fluid volume is due to the external pressure difference, and that is as we have just argued equal to the drag. We may however compare the drag with the force that the jet of fluid in the pipe would exert if it hit a wall (see page 265). This force equals the total rate of momentum discharge through the pipe and is the product $\rho_0 U Q = \rho_0 U^2 \pi a^2$ of the momentum density $\rho_0 U$ and the volume discharge rate $Q = \pi a^2 U$. Using (18-28) we find a dimensionless measure of the drag (the drag coefficient)

$$\frac{\mathcal{D}}{\rho_0 U Q} = \frac{8\eta L}{\rho_0 U a^2} = \frac{1}{2} \cdot \frac{L}{2a} \cdot \frac{64}{\mathsf{Re}} \ . \tag{18-30}$$

The factor $L/2a$ is the length of the pipe in units of the diameter and it expresses that the drag always grows linearly with the length of the pipe (due to longitudinal symmetry). The factor $64/\mathsf{Re}$ expresses in dimensionless form that the jet force grows quadratically with velocity whereas the drag itself only grows linearly.

Dissipation

Since there is no loss of kinetic energy from the control volume, the total power of all the forces acting on the fluid, internal and external, must vanish. The no-slip condition requires the velocity field to vanish at the wall, implying that the shear stress from the pipe wall performs no work on the fluid. The only external forces that perform work are the pressure forces at the ends of the pipe. But because the pressure is constant over the pipe cross section, one may calculate its rate of work on a length L of the pipe from the force $\pi a^2 \Delta p$ times the average velocity U,

$$P = \pi a^2 \Delta p \, U = 8\pi\eta U^2 L \ . \tag{18-31}$$

This must exactly equal the power loss due to the internal friction forces in the fluid, *i.e.* the power dissipated into heat (see problem 18.26).

Example 18.6.3: A hypodermic syringe has a cylindrical chamber with a diameter of about 1 cm and a hollow needle with an internal diameter of about $2a \approx 0.5$ mm. During an injection, the liquid (for example water) is gently pressed through the needle at a rate of about $Q \approx 0.5$ cm^3/s. The average fluid velocity in the needle becomes $U \approx 2.5$ m/s, corresponding to a Reynolds number $\mathsf{Re} \approx 1500$, which is in the laminar region somewhat below the onset of turbulence. One is thus justified in using the Poiseuille solution for the flow through the needle.

The pressure gradient necessary to drive this flow is found from (18-23) and becomes rather large, $G \approx 3$ bar/m. For a needle of length $L \approx 5$ cm the pressure drop is $\Delta p \approx 0.15$ bar $= 15,000$ Pa. The analogous viscous pressure drop in the fluid chamber is only about 0.1 Pa and can be ignored.

To overcome the pressure drop in the needle, one must act with a force of about $\mathcal{D} \approx 1.13$ N on the piston, corresponding to the weight of 113 g, a force which must be added to the force arising from friction between the piston and the wall of the fluid chamber. The force due to the acceleration of the fluid can be calculated from the rate of momentum loss through the exit, $\rho_0 U Q \approx 0.001$ N, and can likewise be ignored.

The dissipated power is $P \approx 2.9$ W. If it takes $\Delta t = 10$ seconds to carry out the injection of 5 cc fluid, the work performed against viscosity alone is about $W = \mathcal{D} U \Delta t \approx 29$ J, all of which is dissipated into heat in the fluid. This amount of heat raises the temperature of $M \approx 5$ g water (with a specific heat of about $c_P \approx 4.2$ J$/K/g$) by $\Delta T = W/c_P M \approx 1.4°$. The patient will hardly feel it!

Again we may obtain a dimensionless measure of the dissipated power by comparing it with the rate of kinetic energy flow through the pipe,

$$\frac{P}{\frac{1}{2}\rho_0 U^2 Q} = \frac{L}{2a} \cdot \frac{64}{\mathsf{Re}} \ . \tag{18-32}$$

Apart from a factor 1/2, this is the same as the dimensionless measure for the drag.

* 18.7 Phenomenology of turbulent pipe flow

It was Osborne Reynolds himself who in 1883 first investigated the nature of turbulent pipe flow[2]. Laminar flow is as mentioned only possible up to a certain critical value of the Reynolds number, beyond which turbulence sets in. Before turbulence is fully developed there is, however, first a transition region characterized by various types of instabilities and intermittent behavior. After turbulence has become fully established there may even be more than one stage, where different physical processes dominate the turbulent character of the flow. Although turbulent pipe flow is still an unsolved problem (in the sense that laminar flow is solved), there exist efficient semi-empirical expressions for the general behavior as a function of Reynolds number.

Reynolds number

In fully developed turbulence the true velocity field varies rapidly in time as well as from place to place in the tube. If dye is injected into the fluid, it rapidly spreads over the whole volume, quite different from laminar flow where it makes orderly streaks. The volumetric discharge rate Q is nevertheless expected to be relatively steady in turbulent flow, albeit with some fluctuations. The bulk velocity calculated from the discharge rate,

$$U = \frac{Q}{\pi a^2} \ , \tag{18-33}$$

is thus a measure of the average rate at which the plug of turbulent fluid progresses down the pipe. As before we may define the Reynolds number to be

$$\mathsf{Re} = \frac{2aU}{\nu} \ . \tag{18-34}$$

Turbulence typically sets in around $\mathsf{Re} \approx 2000 - 4000$, depending on the conditions under which this region is approached, with the nominal value being 2300. For a smooth pipe under *very* carefully controlled conditions, the transition to turbulence can in fact be delayed until a Reynolds number of the order of 100,000. Above that value, the flow is so sensitive to disturbances that it becomes practically impossible to avoid turbulence, even if the Poiseuille solution in fact may be formally stable for all values of the Reynolds number.

[2]Reynolds reference

Friction factor

Intuitively, one expects that turbulence causes increased resistance to the flow and therefore requires a higher pressure drop Δp than laminar flow in order to obtain the same rate of discharge under steady conditions. The turbulent drag $\mathcal{D} = \pi a^2 \Delta p$ and dissipation $P = \mathcal{D}U$ are accordingly also expected to be larger than the laminar drag (18-28) and dissipation (18-31). Since the Reynolds number (or a function of the Reynolds number) is the only dimensionless quantity that may be constructed from the discharge rate or the average velocity (problem 18.10) we may always write the drag in the form

$$\boxed{\mathcal{D} = 8\pi\eta U L f(\mathsf{Re})}\ , \tag{18-35}$$

where $f(\mathsf{Re})$ is a dimensionless function of the Reynolds number, which we shall call the *friction factor*. It is evidently *anchored* with the value $f(\mathsf{Re}) = 1$ in laminar flow, and as we shall see below it grows monotonically with the Reynolds number after the transition to turbulence.

Comparing with the total rate of momentum discharge $\rho_0 U Q$ from the tube we obtain as in (18-30) a dimensionless measure of the drag

$$\frac{\mathcal{D}}{\rho_0 U Q} = \frac{1}{2} \cdot \frac{L}{2a} \cdot \frac{64}{\mathsf{Re}} f(\mathsf{Re})\ . \tag{18-36}$$

Henri-Philibert-Gaspard Darcy (1803-1858). *French engineer, pioneered the understanding of fluid flow through porous media and established Darcy's law which is used in hydrogeology.*

The last part of this expression is the *Darcy friction factor (1857)*,

$$f_{\text{Darcy}}(\mathsf{Re}) = \frac{64}{\mathsf{Re}} f(\mathsf{Re})\ . \tag{18-37}$$

In the technical literature this is traditionally the friction factor of choice. We shall mostly stick to the definition (18-35), mainly because it is universally anchored in the laminar flow value, $f(\mathsf{Re}) = 1$[3]. Generally (as we shall see below) the Darcy friction factor approaches a constant for infinite Reynolds number, except for perfectly smooth pipes. It is thus anchored in the region of extremely turbulent flow, but the limiting value $f_{\text{Darcy}}(\infty)$ is not universal.

In laminar flow the pressure gradient $G = \Delta p/L$ is directly proportional to the volume discharge, so that the viscosity $a^4G/8Q = \eta$ calculated from the Hagen-Poiseuille law (18-22) will be a constant independently of the volume discharge. For turbulent flow we find instead from (18-35) using $\Delta p = \mathcal{D}/\pi a^2$

$$\frac{\pi a^4 G}{8Q} = \eta f(\mathsf{Re})\ . \tag{18-38}$$

This shows that the $\eta^* = \eta f(\mathsf{Re})$ is the effective volume discharge dependent viscosity we would obtain if we indiscriminately used the Poiseuille formalism in the turbulent regime.

[3] It is also closer to what Reynolds himself did.

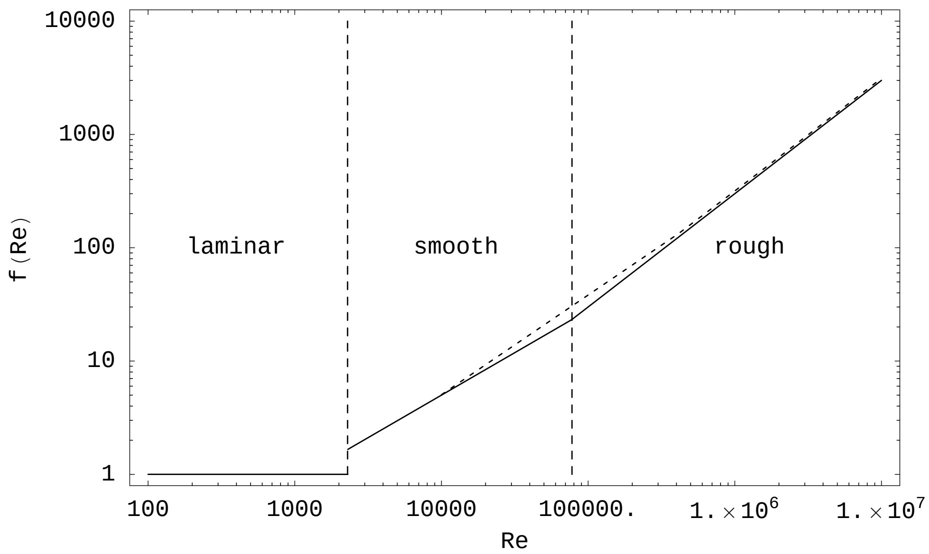

Figure 18.1: *Schematic behavior of the friction factor* $f(\mathsf{Re})$ *as a function of Reynolds number* Re *for a pipe with roughness* $\epsilon/2a = 10^{-3}$ *(where* ϵ *is a measure for the height of the small protrusions in the wall). The transition from laminar to smooth-pipe turbulent flow happens around* $\mathsf{Re} \approx 2300$ *but the friction factor is not too well-defined for* $2000 \lesssim \mathsf{Re} \lesssim 4000$*. The transition from smooth-pipe turbulence to rough-pipe turbulence happens in this case for* $\mathsf{Re} \approx 77,000$*. It is quite soft and the behavior in the two regions is better described by the interpolation (dashed curve).*

The conclusion that the complex behavior of turbulent fluid flowing through a pipe can be summarized by a single function of the Reynolds number was definitely not clear from the outset. Since the parameters, Q, a, η and G, can all be determined from measurements, the friction factor is an experimentally accessible quantity for nearly all values of the Reynolds number. A huge amount of theoretical and experimental work has been done over the years in order to determine the friction factor, but we shall here only summarize its overall behavior and in later chapters present some of the theory behind (see [36, ch. 6] for an extensive technical discussion).

Smooth pipe case

The behavior of the friction factor beyond the laminar region depends on the character of the inner surface of the pipe. For a perfectly smooth surface a decent approximation was given by Blasius in 1911, in which the friction factor grows like the 3/4'th power of the Reynolds number,

$$f(\mathsf{Re}) \approx \lambda_0 \, \mathsf{Re}^{\frac{3}{4}} \,, \tag{18-39}$$

with $\lambda_0 \approx 0.005$. Although this function crosses the laminar value $f(\mathsf{Re}) = 1$ for $\mathsf{Re} \approx 1200$, the actual transition to turbulence happens as mentioned somewhat later for $\mathsf{Re} \approx 2300$ (see fig. 18.1). In the transition region the friction factor is in fact not so well-defined as in the laminar and fully turbulent regions because of intermittent shifts between the two types of flow.

One may wonder whether the smooth pipe expression has any relevance except for glass pipes that in fact are quite smooth. Lots of industrially produced pipes are for example made from rubber, plastic, iron, or concrete with differing degrees of roughness at their inner surfaces. But it turns out that any not too rough pipe will tend to behave approximatively like a perfectly smooth pipe in some region beyond the transition to turbulence. The reason is that when turbulence sets in, the no-slip condition still requires the fluid velocity to vanish near the wall of the pipe. This leads to the formation of boundary layers which screen the bulk of the flow from the influence of the roughness of the inner pipe surface, and the pipe appears to be smooth.

The boundary layers, however, become thinner and the screening less important for very high Reynolds numbers. Above a certain value that depends on the character of the roughness, typically $\mathsf{Re} \gtrsim 100,000$, the smooth pipe approximation completely loses its usefulness.

Example 18.7.1 (Water pipe cont'd): A quite normal use of household water was shown in example 18.6.2 to lead to a Reynolds number of about $\mathsf{Re} \approx 11,600$, which is well inside the turbulent regime, though not in the rough pipe region. From the smooth pipe formula (18-39) we find the friction factor $f(11,600) = 5.6$. The pressure gradient must therefore be 5.6 times the Hagen-Poiseuille value (which is 140 $\mathsf{Pa/m}$), or $G \approx 780$ $\mathsf{Pa/m}$. Drag and dissipation are similarly augmented.

Turbulence makes the pipes hiss or "sing" when you tap water at full speed, though most of the noise probably comes from the narrow passages of the faucet, where the water speed and Reynolds number are highest, and the big drop from main pressure to atmospheric takes place.

Rough pipe limit

In the limit of extremely high Reynolds number, the character of the flow tends to be controlled by the unavoidable roughness of the inner pipe surface, rather than by the tiny remaining viscous friction in the fluid. The fluid literally slams into the irregularities of the pipe surface at high speed, creating a turbulent flow for which the pressure gradient does not depend strongly on the actual viscosity (even if it in the end owes its existence to viscosity!).

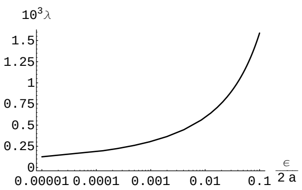

Plot of the asymptotic coefficient λ times 10^3 as a function of roughness $\epsilon/2a$.

But that is only possible if the friction factor is directly proportional to the Reynolds number, such that we get the same η-dependence on both sides of (18-35). The asymptotic behavior of the friction factor is thus expected to be

$$f(\mathsf{Re}) \approx \lambda\, \mathsf{Re}\ , \tag{18-40}$$

where the constant of proportionality $\lambda = f_{\text{Darcy}}(\infty)/64$ depends rather weakly on the actual roughness of the pipe surface, measured for example by the typical height $\epsilon \ll 2a$ of the protrusions and irregularities of the surface. The following semi-empirical expression summarizes its behavior

$$\lambda = \frac{0.012}{\left(1 - 1.76 \log_{10} \dfrac{\epsilon}{2a}\right)^2} \ . \tag{18-41}$$

Rubber, for example, has $\epsilon \approx 0.01$ mm, so that for a 10 mm rubber hose we get $\epsilon/2a \approx 0.001$ and $\lambda = 0.0003$. The smooth and rough pipe expressions cross each other at $\mathsf{Re} = (\lambda_0/\lambda)^4$, which in this case becomes $\mathsf{Re} = 77,000$.

The transition from smooth to rough pipe turbulence is rather soft and certainly not as sharp as the transition from laminar to turbulent flow (see fig. 18.1). Various interpolating semi-empirical expressions and diagrams useful for engineering design purposes have been constructed for the detailed behavior of the Darcy friction factor in the two regimes and may be found in the technical literature, for example [36, p. 348].

* 18.8 Down the drain, again

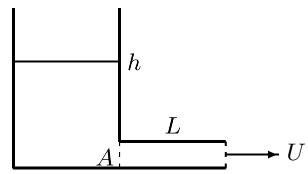

The water leaving the cistern through a narrow pipe experiences a drag from the pipe.

Returning to the draining of a cistern (section 16.8), we are now able to take into account the slowing down of the flow due to viscosity. For a sufficiently large cistern, and a sufficiently narrow and long pipe, the flow through the drain pipe is essentially steady, and we may as before apply kinetic energy balance (section 16.6) to find the terminal average velocity in the pipe in the laminar as well as the turbulent regimes.

Laminar drain

Taking the control volume to be all the water in the cistern and the pipe, the material rate of change of the kinetic energy is under steady conditions entirely due to the loss of kinetic energy through the exit of the drain pipe. Writing the Poiseuille profile (18-21) in the form, $v_z(r) = 2U(1 - r^2/a^2)$, we find

$$\frac{\delta \mathcal{T}}{\delta t} = \int_0^a \frac{1}{2}\rho_0 v_z(r)^2 \cdot v_z(r)\, 2\pi r\, dr = \rho_0 \pi a^2 U^3 \ , \tag{18-42}$$

where U is the average velocity. This is actually twice the estimate used in (16-51), but such correction factors are to be expected, because we now take into account the variation in the velocity field across the pipe. On the right hand side of the kinetic energy balance (16-36) we must calculate the total power of all the forces acting on the fluid. Using Leonardo's law (16-47), we obtain

$$P = g_0 \rho_0 h \pi a^2 U - 8\pi\eta U^2 L \ , \tag{18-43}$$

where the first term is the power of gravity on the water in the cistern, and the second the dissipation in the drain pipe (18-31). The power of atmospheric pressure on the two open surfaces vanishes as before, also because of Leonardo's law.

Equating these two expressions we get a quadratic equation for the terminal velocity,

$$2U^2 + \frac{16\nu L}{a^2} U = 2g_0 h \tag{18-44}$$

where ν is the kinematic viscosity. The solution is

$$U = \sqrt{g_0 h + \left(\frac{4\nu L}{a^2}\right)^2} - \frac{4\nu L}{a^2} \tag{18-45}$$

For $\nu \to 0$ the solution becomes $U = \sqrt{g_0 h}$, which is a factor $\sqrt{2}$ smaller than the Torricelli expression $U_0 = \sqrt{2g_0 h}$ for nearly ideal flow (section 15.5). This mismatch should however not cause worry, because the parabolic Poiseuille solution is *not* supposed to work in the limit $\nu \to 0$ where $\mathsf{Re} \to \infty$. Long before this limit is reached, the laminar flow is replaced by turbulence with a different velocity distribution and drag.

Example 18.8.1: A bag of blood with a height of 20 cm is drained through a long vertical plastic tube of length $L = 30$ cm with internal diameter $2a = 3$ mm. The density of blood is like that of water and its viscosity $\eta \approx 4 \times 10^{-3}$ Pa s. Since the total drop height is $h = 50$ cm, the terminal velocity becomes $U \approx 1$ m/s, which is about half the free fall velocity. The corresponding Reynolds number is $\mathsf{Re} \approx 700$, well below the onset of turbulence.

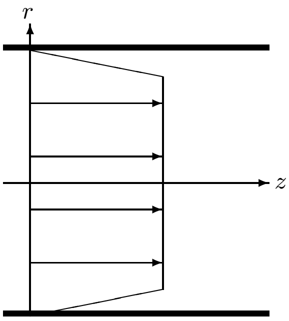

Assumed velocity profile for fully developed turbulent flow through a circular pipe. Apart from thin boundary layers (which we ignore), the velocity field is approximatively constant across the pipe.

Turbulent drain

The calculation in the turbulent case proceeds in much the same way, except that we do not know the actual velocity distribution in the pipe. We have formerly mentioned the existence of boundary layers in turbulent pipe flow, but we shall for simplicity assume that the bulk of the turbulent flow proceeds through the pipe as a *turbulent plug* with roughly the same average speed across the pipe.

This changes the rate of loss of kinetic energy to half of (18-42)

$$\frac{\delta \mathcal{T}}{\delta t} \approx \frac{1}{2}\rho_0 U^2 \cdot \pi a^2 U = \frac{1}{2}\rho_0 \pi a^2 U^3 \ . \tag{18-46}$$

The total power of all the forces is essentially unchanged except for inclusion of the friction factor in the dissipative term,

$$P = g_0 \rho_0 h A_0 U_0 - \mathcal{D} U = g_0 \rho_0 h \pi a^2 U - 8\pi\eta U^2 L f(\mathsf{Re}) \ . \tag{18-47}$$

Equating the two we obtain the following equation for U

$$U^2 + \frac{16\nu U L}{a^2} f\left(\frac{2aU}{\nu}\right) = 2g_0 h \ . \tag{18-48}$$

Were it not for the second term due to turbulence on the left hand side, we would indeed recover Torricelli's law, $U = U_0 = \sqrt{2g_0 h}$. In the general case this equation has to be solved numerically (see problem 18.18).

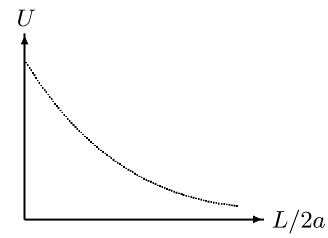

Turbulent terminal speed as a function of pipe length. For sufficiently long pipes the flow becomes laminar.

In the limit of $\nu \to 0$ we may use the rough pipe form of the friction factor (18-40), and the above equation then becomes a simple quadratic viscosity-independent equation with the solution

$$U = \sqrt{\frac{2g_0 h}{1 + 64\lambda \dfrac{L}{2a}}} \; . \tag{18-49}$$

Here we recognize the Darcy friction factor $f_{\mathrm{Darcy}}(\infty) = 64\lambda$. Clearly, Torricelli's result is only obtained for short pipes, obeying $L \ll 2a/64\lambda$, whereas for long pipes, $L \gg 2a/64\lambda$, the terminal velocity falls as $1/\sqrt{L}$. Eventually this will bring the Reynolds number down into the smooth pipe and laminar regions.

Example 18.8.2 (Barrel of wine, cont'd): For the barrel of wine (example 16.8.1 on page 273) which empties through a wooden spout of length $L = 20$ cm and diameter $2a = 5$ cm the Reynolds number is about 300,000, well into the rough pipe region. Disregarding entry corrections and assuming a roughness of $\epsilon \approx 0.5$ mm, we find $\lambda \approx 0.0006$ and $64\lambda L/2a \approx 0.15$. Thus the Toricelli value for the exit velocity is only reduced by about 15 % by turbulence.

18.9 Circulating cylindrical flow

In the cylindrical geometry there is another exact solution with maximal symmetry, in which the fluid circles around the cylinder axis with a velocity field of the form,

$$\boldsymbol{v} = v_\phi(r)\boldsymbol{e}_\phi \; , \tag{18-50}$$

where $\boldsymbol{e}_\phi$ is the tangential unit vector in cylindrical coordinates (see section 2.7). The field lines are concentric circles, and the field is evidently invariant under rotations around the cylinder axis and translations along it.

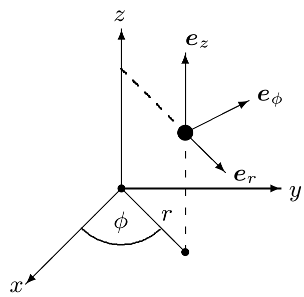

Cylindrical coordinates and basis vectors (see section 2.7).

General solution

In this case the simplest approach is to make use of the gradient in cylindrical coordinates (2-57) to calculate its "tensor product" with the velocity

$$\boldsymbol{\nabla v} = (\boldsymbol{e}_r\nabla_r + \boldsymbol{e}_\phi\nabla_\phi + \boldsymbol{e}_z\nabla_z)v_\phi(r)\boldsymbol{e}_\phi = \boldsymbol{e}_r\boldsymbol{e}_\phi\frac{dv_\phi}{dr} - \boldsymbol{e}_\phi\boldsymbol{e}_r\frac{v_\phi}{r} \; . \tag{18-51}$$

Here we have used the orthogonality of the basis vectors and that $\nabla_\phi \boldsymbol{e}_\phi = -\boldsymbol{e}_r/r$. Since this tensor has only off-diagonal components, its trace $\mathrm{Tr}[\boldsymbol{\nabla v}] = \mathsf{div}\,\boldsymbol{v} = 0$, in agreement with the elementary observation that streamlines neither diverge nor converge. Dotting from the left with $\boldsymbol{v}$ we find the convective acceleration

$$(\boldsymbol{v}\cdot\boldsymbol{\nabla})\boldsymbol{v} = \boldsymbol{v}\cdot(\boldsymbol{\nabla v}) = -\boldsymbol{e}_r\frac{v_\phi^2}{r} \; .$$

It does not vanish because the flow continually changes direction. The acceleration in a circular motion with velocity v_ϕ is indeed directed radially inwards and of size v_ϕ^2/r.

Finally, we obtain in a similar way the Laplacian by dotting (18-51) with $\boldsymbol{\nabla}$ from the left

$$\begin{aligned}\boldsymbol{\nabla}^2\boldsymbol{v} = \boldsymbol{\nabla}\cdot(\boldsymbol{\nabla}\boldsymbol{v}) &= (\boldsymbol{e}_r\nabla_r + \boldsymbol{e}_\phi\nabla_\phi + \boldsymbol{e}_z\nabla_z)\cdot\left(\boldsymbol{e}_r\boldsymbol{e}_\phi\frac{dv_\phi}{dr} - \boldsymbol{e}_\phi\boldsymbol{e}_r\frac{v_\phi}{r}\right)\\ &= \boldsymbol{e}_\phi\frac{d^2v_\phi}{dr^2} + \boldsymbol{e}_\phi\frac{1}{r}\frac{dv_\phi}{dr} - \boldsymbol{e}_\phi\frac{v_\phi}{r^2} = \boldsymbol{e}_\phi\frac{d}{dr}\left(\frac{1}{r}\frac{d(rv_\phi)}{dr}\right) .\end{aligned}$$

The rewriting of the last expression is done for later convenience. The above result could of course also have been derived from the cylindrical representation of the Laplacian (2-60), using that $\partial^2\boldsymbol{e}_\phi/\partial\phi^2 = -\boldsymbol{e}_\phi$.

Putting these results together the Navier-Stokes equation (18-4) becomes,

$$-\rho_0\boldsymbol{e}_r\frac{v_\phi^2}{r} = -\boldsymbol{\nabla}p^* + \eta\,\boldsymbol{e}_\phi\frac{d}{dr}\left(\frac{1}{r}\frac{d(rv_\phi)}{dr}\right) , \tag{18-52}$$

and projecting it on the three cylindrical basis vectors, $\boldsymbol{e}_r$, $\boldsymbol{e}_\phi$, and $\boldsymbol{e}_z$, we obtain

$$-\rho_0\frac{v_\phi(r)^2}{r} = -\frac{\partial p^*}{\partial r} , \tag{18-53a}$$

$$0 = -\frac{1}{r}\frac{\partial p^*}{\partial\phi} + \eta\frac{d}{dr}\left(\frac{1}{r}\frac{d(rv_\phi)}{dr}\right) , \tag{18-53b}$$

$$0 = -\frac{\partial p^*}{\partial z} . \tag{18-53c}$$

From the last equation it follows that the effective pressure is independent of z, and from the second equation we see by differentiating after ϕ that $\partial^2p^*/\partial\phi^2 = 0$, which means that p can at most be linear in ϕ, *i.e.* of the form $p^* = p_0(r)+p_1(r)\phi$. But here we must require $p_1 = 0$, for otherwise the pressure would have different values for $\phi = 0$ and $\phi = 2\pi$, and that is impossible. For this reason the pressure cannot depend on ϕ but only on r, and thus it disappears completely from (18-53b).

With the pressure out of the way, the integration of (18-53b) has become almost trivial. The general solution is

$$v_\phi = Ar + \frac{B}{r} , \tag{18-54}$$

where A and B are integration constants. The first equation (18-53a) expresses that there is a positive radial pressure gradient which supplies the centripetal force necessary to keep the fluid in its circular motion. Inserting the general solution into (18-53a) and integrating over r, we find the effective pressure

$$\frac{p^*}{\rho_0} = C + \frac{1}{2}A^2r^2 - \frac{1}{2}\frac{B^2}{r^2} + 2AB\log r , \tag{18-55}$$

where C is a third integration constant.

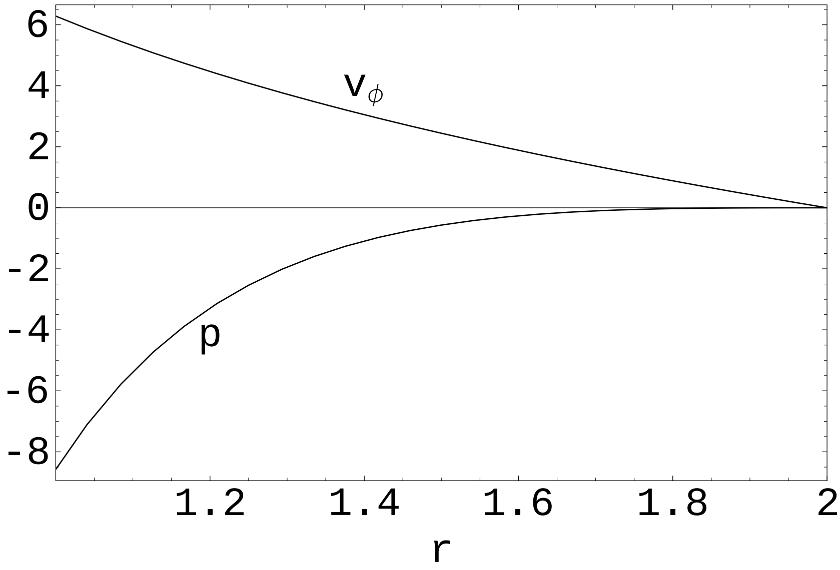

Figure 18.2: *Plot of velocity (18-56) and pressure (18-57) for the spindle-driven Couette flow as a function of radial distance r. The parameters are $a = 1$, $b = 2$, and $\Omega = 2\pi$. The pressure rises towards the outer cylinder (where it is defined to vanish) and thereby provides the centripetal force necessary for the circular motion.*

18.10 Couette flow between rotating cylinders

Maurice Couette (1858–1943). *French scientist. Very little seems to be known about him.*

Suppose the fluid is contained between two long coaxial material cylinders with the innermost having radius a and outermost radius $b > a$. This problem was solved by Couette (1890), but today *Couette flow* is often used to denote any kind of motion-driven laminar flow, for example also laminar channel flow between moving parallel plates (p. 287).

Here we shall for simplicity only study the case where the outer cylinder is held fixed and the inner cylinder rotates like a spindle with constant angular velocity Ω. The boundary conditions, $v_\phi(a) = a\Omega$ and $v_\phi(b) = 0$, then determine A and B, so that the velocity profile becomes

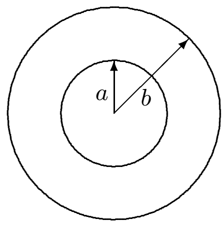

Couette flow geometry.

$$\boxed{v_\phi = \frac{a^2\Omega}{r}\frac{b^2 - r^2}{b^2 - a^2}} . \tag{18-56}$$

Evidently, it is of the general form (18-54) and fulfills the boundary conditions.

The velocity field does not depend on the viscosity of the fluid, a feature that can be traced back to the vanishing of the convective tangential acceleration in (18-53b).

Pressure and shear stress

The effective pressure is found from (18-55)

$$p^* = p_0 + \frac{1}{2}\rho_0 \left(\frac{a^2\Omega}{b^2 - a^2}\right)^2 \left(r^2 - \frac{b^4}{r^2} + 4b^2 \log\frac{b}{r}\right) , \tag{18-57}$$

where p_0 is its value at the outer cylinder.

From (18-51) it follows that the only non-vanishing shear stress component is

$$\sigma_{\phi r} = \eta(\boldsymbol{e}_\phi \cdot (\boldsymbol{\nabla}\boldsymbol{v}) \cdot \boldsymbol{e}_r + \boldsymbol{e}_r \cdot (\boldsymbol{\nabla}\boldsymbol{v}) \cdot \boldsymbol{e}_\phi) = \eta\left(\frac{dv_\phi}{dr} - \frac{v_\phi}{r}\right) , \tag{18-58}$$

or upon insertion of the Couette solution (18-56)

$$\sigma_{\phi r} = -2\eta\,\Omega\frac{a^2b^2}{b^2 - a^2}\frac{1}{r^2} \tag{18-59}$$

It represents the friction between the layers of circulating fluid, and the sign is negative because the fluid *outside* the radius r acts as a brake on the motion of the fluid *inside* (which has normal $\boldsymbol{e}_r$).

Torque and dissipation

In order to maintain the steady rotation of the inner cylinder it is necessary to act on it with a moment of force or torque $\mathcal{M}_z$ (and with an opposite moment at the outer cylinder). Multiplying the shear stress with the moment arm r and the area $2\pi rL$ of the cylinder at r, we finally obtain the torque with which the fluid *inside* r acts on the fluid *outside*,

$$\mathcal{M}_z = r\,(-\sigma_{\phi r})2\pi rL = 4\pi\eta\Omega L\frac{a^2b^2}{b^2 - a^2} . \tag{18-60}$$

It is independent of the radial distance r. We could have foreseen that: in steady flow the total moment of force on a control volume of fluid between any two cylindrical surfaces has to vanish, and consequently it must be the same on all cylindrical surfaces.

The rate of work that must be done against the torque to keep the inner cylinder rotating against the friction from the fluid is obtained by multiplying the stress $-\sigma_{\phi r}$ with the velocity $r\Omega$ and "integrating" over the cylinder,

$$P = (-\sigma_{\phi r})\; r\Omega\; 2\pi rL = \mathcal{M}_z\Omega = 4\pi\eta\Omega^2 L\frac{a^2b^2}{b^2 - a^2} . \tag{18-61}$$

Since the kinetic energy of the fluid is constant in steady flow and since no fluid enters or leaves the system, this must equal the rate of energy dissipation in the fluid.

This is exploited in the Couette viscometer by measuring the extra motor power necessary to drive the inner cylinder at constant angular velocity. Another possibility is to hang the inner cylinder in a torsion wire and rotate the outer cylinder at constant angular velocity (a more stable situation, see page 326). The torsional rigidity (page 179) of the wire may be determined from the period of free oscillations of the inner cylinder with an empty chamber. When the chamber is filled with viscous fluid there will arise a torque on the inner cylinder, which is counteracted by the torsion in the wire so that at equilibrium a certain deflection angle is obtained. Measuring the deflection angle then leads to a value for the viscosity (problem 18.23).

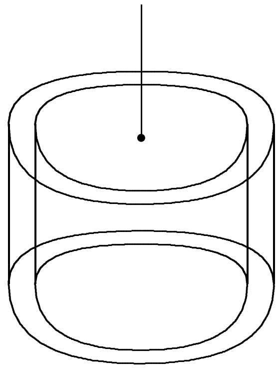

Sketch of torsion wire Couette viscometer.

Unloaded journal bearing

In a lubricated *journal bearing* a liquid, say oil, is trapped in a tiny gap between a rotating shaft (or journal) and its bearing (or bushing)[4]. Normally such systems carry a load which brings the shaft off-center (see section 23.4) but here we shall assume that the journal and its bushing are concentric cylinders, such that we may apply the Couette formalism in the limit of very small distance $d = b - a \ll a$ between the cylinders. We find to lowest order in d and in the distance $s = r - a$ from the shaft

$$v_\phi = a\Omega\left(1 - \frac{s}{d}\right) . \qquad (18\text{-}62)$$

The velocity field is linear in s, just as for planar Couette flow. This is not particularly surprising since the tiny gap between the cylinders look very much like the gap between parallel plates. The natural definition of the Reynolds number is correspondingly

$$\mathsf{Re} = \frac{\Omega a d}{\nu} , \qquad (18\text{-}63)$$

and we expect turbulence to arise for $\mathsf{Re} \gtrsim 2000$, as in the planar case.

The pressure is found from (18-57) by expanding the logarithm to third order in s and d, and it becomes in the leading approximation,

$$p = p_0 - \frac{1}{3} a d\Omega^2 \left(1 - \frac{s}{d}\right)^3 . \qquad (18\text{-}64)$$

The pressure variation across the gap is proportional to the size of the gap and thus normally tiny, unless the quadratic growth with angular velocity overwhelms it. The dissipation becomes on the other hand to lowest order in d,

$$P = \frac{2\pi\eta\Omega^2 a^3 L}{d} . \qquad (18\text{-}65)$$

It is inversely proportional to the thickness of the layer of fluid and grows like the pressure variation quadratically with the angular velocity. This is why even a lubricated bearing may burst into flames at high rpm's.

[4]Technical language is sometimes quite peculiar and flowery, reflecting its long use.

Example 18.10.1 (Burning bush): Consider a vertical wooden shaft in a wooden bushing with diameter $2a = 10$ cm, such as could have been used in an old water mill. Let the gap be $d = 1$ mm and let the lubricant be heavy grease with $\eta \approx 10$ Pa s, corresponding to $\nu \approx 0.01$ m^2/s. The power dissipated per unit of lubricant volume is

$$\frac{P}{2\pi a L d} = \frac{\eta \Omega^2 a^2}{d^2} . \tag{18-66}$$

For a modest speed of one rotation per second, $\Omega \approx 2\pi/s$ with a Reynolds number of $\mathsf{Re} \approx 0.06$, this comes to about 1 J/cm^3/s. If the mill rotates 10 times faster because of torrential rains, this number becomes instead 100 J/cm^3/s with a Reynolds number of 0.6. Since wood is a bad heat conductor, the grease may ignite in a matter of minutes even taking into account that its viscosity decreases with temperature.

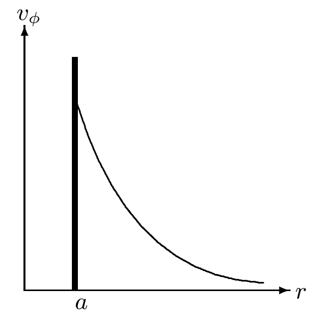

Characteristic $1/r$ velocity profile of spindle-driven vortex.

Spindle-driven vortex

Suppose a long cylindrical spindle of radius a is inserted into an infinite sea of fluid, and that the spindle is rotated steadily with constant angular velocity Ω. Provided the spindle does not rotate so fast that it creates turbulence, the flow will eventually become steady with an azimuthal velocity field that may be found from the Couette solution with $b \to \infty$,

$$v_\phi = \frac{a^2 \Omega}{r} , \qquad p^* = -\frac{1}{2}\rho_0 \frac{a^4 \Omega^2}{r^2} . \tag{18-67}$$

The effective pressure has been normalized to vanish at infinity.

In a gravitational field g_0 pointing downwards along the cylinder axis the effective pressure is also given by $p^* = p + \rho_0 g_0 z$, where p is the true pressure. If the fluid is a nearly ideal liquid, the true pressure at an open surface must equal the (constant) air pressure at the interface, just as in hydrostatics. Choosing the asymptotic level of fluid to be $z = L$, we therefore obtain the following shape of the surface,

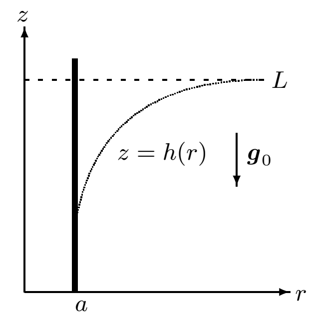

Open liquid surface $z = h(r)$ of a spindle-driven vortex in constant gravity varies like $1/r^2$.

$$z = L + \frac{p^*}{\rho_0 g_0} = L - \frac{\Omega^2 a^4}{2 g_0 r^2} . \tag{18-68}$$

This is quite different from the parabolic shape of the liquid surface in a rotating bucket (page 110).

Example 18.10.2: A spindle with radius $a = 1$ cm making 10 turns per second, corresponding to $\Omega = 63$ s^{-1}, would make a depression in the liquid surface with maximum $L - h(a) = 2$ cm at the spindle.

The rule about continuity of pressure across any surface is only strictly valid in hydrostatics (in the absence of surface tension), whereas in hydrodynamics it is instead the full stress vector that is required to be continuous across the open surface. Since the Couette solution has a finite shear stress $\sigma_{\phi r}$ everywhere, the stress vector cannot vanish exactly at the open liquid surface, but only approximatively in the limit of vanishing viscosity. The structure of driven as well as free vortices will be analyzed in detail in chapter 21.

∗ 18.11 Secondary flow and Taylor vortices

Real machinery cannot be infinite in any direction. Suppose the cylinders are capped with plates fixed to the outer non-rotating cylinder so that only the inner cylinder rotates. The no-slip condition forces the rotating fluid to slow down and come to rest not only at the outer cylinder, but also at both the end caps, implying that the assumption about a simple circulating flow (18-54) with its z-independent azimuthal velocity $v_\phi(r)$ cannot be right everywhere. In fact it cannot be right anywhere! Clean Couette flow is like clean Poiseuille flow an idealization that can only be approximately realized far from the ends of the apparatus. *Secondary flow* with non-vanishing radial and longitudinal velocity components, v_r and v_z, will have to arise near the container walls in order to satisfy the no-slip boundary conditions at the end caps.

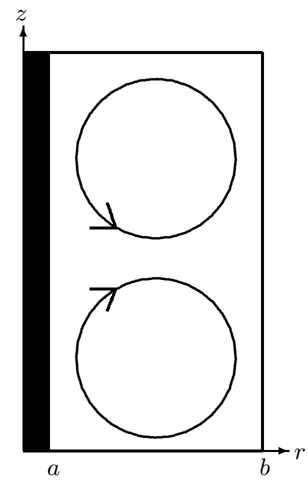

Sketch of the secondary flows that arise in a Couette apparatus as a consequence of its finite longitudinal size. Both at the bottom and the top end caps fluid is driven towards the central region because of the no-slip boundary conditions.

Direction of secondary flow

We shall to begin with assume that the length of the apparatus is comparable to the gap, say $L \approx 2d$, and that the gap is completely filled with fluid without open surfaces. In the bulk of the fluid, the Couette solution is still a good approximation, and the main job of the (effective) pressure is here to provide centripetal force for the circulating fluid as shown by the radial gradient (18-53a).

The longitudinal pressure gradient $\nabla_z p^*$ determines how rapidly the pressure can vary in the z-direction, and from the z-component of the full Navier-Stokes equation (18-4) we obtain

$$\nabla_z p^* = -\rho_0(\boldsymbol{v}\cdot\boldsymbol{\nabla})v_z + \eta\boldsymbol{\nabla}^2 v_z \ .$$

The right hand side is expected to be small throughout the fluid because the longitudinal velocity v_z must nearly vanish in the Couette bulk flow in the middle of the apparatus and also has to vanish at the bottom end cap (which the fluid coming down from above cannot penetrate). The vertical variation in effective pressure near the bottom is therefore not able to seriously challenge the large values of the centripetally dominated bulk pressure. The pressure is for this reason rather "stiff" as we approach the bottom and remains equal to the pressure in the bulk with only small corrections.

Near the bottom, the still intact bulk pressure will have an inwards directed radial gradient, $-\nabla_r p^*$, capable of delivering the centripetal force to keep the rapidly rotating fluid in the bulk moving in a circle. But the no-slip condition requires the azimuthal velocity to vanish at the bottom, $v_\phi \to 0$ for $z \to 0$, so that the actually required centripetal acceleration $-v_\phi^2/r$ is much smaller there than in the bulk. As a result, the combination of the stiff pressure gradient and the smaller centripetal acceleration gives rise to a net force directed towards the axis, and that force will in turn drive a radial flow inwards along the bottom. The same argument shows that there must also be an inwards flow along the top and since the moving fluid has to go somewhere, it must in the maximally

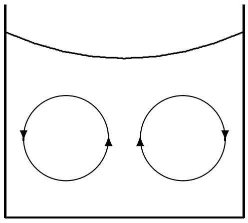

The secondary flow responsible for collecting tea-leaves at the center of the bottom of a stirred cup. Notice the parabolic shape of the surface of the rotating liquid (see page 110).

symmetric case form two oppositely rotating ring-shaped (toroidal) vortices that encircle the axis.

If the axis is vertical and the liquid has an open surface, only a single vortex needs to be formed. It is this kind of secondary flow that drives the tea-leaves along the bottom towards the center of a cup of tea after stirring it. As the above argument shows the flow is independent of the direction of stirring. You cannot, for example, make the tea-leaves move out again by "unstirring" your tea.

Rayleigh's stability criterion

In the above discussion, the cylinder length was assumed to be about the double of the gap size. For a long cylinder, the preceding argument seems to indicate that a secondary flow with two highly elongated "vortices" should form to satisfy the boundary conditions on the end caps, or just one if there is an open surface. Such elongated vortices are, however, unstable and tend to break up in a number of smaller and more circular vortices.

The instability can be understood[5] by analyzing what happens if a fluid particle in the bulk of the rotating fluid is rapidly moved outwards by a fluctuation in the flow. During the move the fluid particle will conserve its angular momentum (because viscous forces do not have enough time to drag it along) and it may arrive in the new position with a speed which is different from the ambient speed of the fluid there. The angular momentum of a unit mass particle in the ambient fluid is rv_ϕ, and if it is constant, $d(rv_\phi)/dr = 0$, then the moved particle fits snugly into its new home with just the right velocity. This is, for example, the case for the spindle-driven vortex (page 324) which has $rv_\phi = \Omega a^2$.

In general the specific angular momentum $r\,|v_\phi|$ of the ambient fluid will not be a constant. If it grows in size with distance, *i.e.* if its absolute value satisfies the inequality (Rayleigh's stability criterion)

$$\frac{d(r\,|v_\phi|)}{dr} > 0 \ , \tag{18-69}$$

then a fluid particle displaced to a slightly larger radius will arrive with its original angular momentum and thus have a smaller velocity than its new surroundings. The inward pressure gradient in the ambient fluid will therefore be larger than required to keep the particle in a circular orbit with lower velocity, and it will be forced back to where it came from. This is, for example, the case if the inner cylinder is held fixed and the outer rotated, because then the velocity must necessarily grow with the radial distance. Such a situation is perfectly stable.

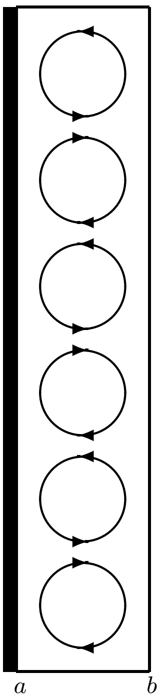

Taylor vortices are toroidal rings of fluid encircling the axis of rotation. In this case both end caps are fixed and the secondary flow must be directed inwards at both top and bottom. That is only possible if an even number of counter-rotating vortices are formed.

Taylor vortices

Conversely, if the above inequality is not fulfilled, the flow may become unstable and reconfigure itself at the first opportunity. For the Couette solution (18-56)

[5]The argument is analogous to the discussion of atmospheric stability on page 70.

we find in general

$$\frac{d(r\,|v_\phi|)}{dr} = -\frac{2a^2\Omega r}{b^2 - a^2}\ , \tag{18-70}$$

which is evidently negative, and more negative the faster it rotates and the narrower is the gap. Viscosity which has been ignored so far will delay the onset of instability, but it requires a more careful analysis to find the precise criterion (see chapter **??**).

For a long cylinder and a sufficiently large angular driving velocity Ω, the flow eventually becomes unstable and a string of ring-shaped vortices form in the gap. They are called *Taylor vortices* in honor of G. I. Taylor who first analyzed the instability giving rise to them. The Taylor vortices are all mutually counter-rotating and match up with the sense of flow dictated by the boundary conditions on the ends.

The formation of secondary flow and the instability leading to ring-shaped Taylor vortices represents a breakdown of the longitudinal symmetry (along z) of the cylinder. The azimuthal symmetry (in ϕ) is to begin with maintained but also breaks down with increasing speed of rotation. The regular Taylor vortices are then replaced by wavy vortices that undulate up and down (in z) while they encircle the axis. Increasing the speed further will increase the number of undulations until the flow finally becomes chaotic and turbulent.

Problems

18.1 Consider a pressure-driven laminar flow between infinitely extended plates moving with constant velocity with respect to each other in the same direction as the pressure gradient. Determine under which conditions the maximal flow velocity will be found in between the plates.

18.2 Determine the planar flow field in the case that pressure gradient is orthogonal to the plate motion.

18.3 Why is it impossible to make a pressure driven planar fluid sheet with an open surface?

18.4 A thin fluid sheet (water) of density ρ_1 and thickness d_1 runs steadily down a fixed vertical plate. Another vertical plate is placed at a distance $d_1 + d_2$ from the first, and there is another fluid (air) in the gap with density ρ_2 and size d_2. Calculate the laminar velocity field in the water and in the air between the plates.

18.5 A fluid flows under the influence of gravity down a plane inclining an angle α with the horizontal. a) Find the laminar flow solution under the assumption that the thickness of the fluid layer is constant (a) everywhere. b) Calculate the true pressure everywhere in the fluid. c) How viscous must the fluid in order for the flow to remain laminar ($\mathsf{Re} < 1000$) when the angle of inclining is $\alpha = 1^\circ$, and the volume rate of discharge (per unit of length orthogonal to the flow) is 0.1 $\mathsf{m^2/s}$.

18.6 Calculate drag and dissipation for pressure driven planar flow.

18.7 Calculate drag and dissipation for gravity driven planar flow with an open surface.

18.8 Derive the basic equations for tubular flow (section 18.5 on page 307) using the formalism of cylindrical coordinates (but not the explicit Laplacian (2-60)).

18.9 Calculate vertical gravity driven water flow through a narrow pipe, and determine the diameter of the pipe as a function of the Reynolds number.

18.10 a) Show that in pipe flow the only dimensionless combination of the parameters Q, a, ρ_0, η is the Reynolds number (up to trivial transformations). b) Can you make another dimensionless parameter by using $G = \Delta p/L$ instead of Q.

18.11 Show that pipe resistance is additive for pipes connected in series and reciprocally additive for pipes connected in parallel.

18.12 A single 1 inch pipe forks into a $\frac{3}{4}$ inch pipe and a $\frac{1}{2}$ inch pipe of the same length. Calculate the ratios between the average velocities in the three pipes under the assumption of laminar flow.

18.13 Calculate drag and dissipation for turbulent pipe flow using the phenomenological description.

18.14 Show that for the Poiseuille profile,

$$\int_0^a v_z(r)^n \, 2\pi r \, dr = \frac{2^{n-1}}{n+1}\rho_0 U^n \pi a^2 \tag{18-71}$$

where U is the average velocity.

18.15 a) Show that for a cylindrical tube with annular cross section with radii $a < b$, the solution is given by the Poiseuille solution (18-20) with

$$A = \frac{G}{4\eta}\frac{b^2 - a^2}{\log b - \log a}$$
$$B = \frac{G}{4\eta}\frac{a^2 \log b - b^2 \log a}{\log b - \log a}$$

b) Determine the drag on the tube per unit of length when a fluid is pressed through the tube under a gradient G.

18.16 Solve Poiseuille flow in an elliptic tube.

18.17 A cylindrical water tank with radius b and initial water height h_0 empties slowly through a vertical cylindrical pipe of length $L >> a$ with radius $a \ll b$. a) Assuming laminar flow in the pipe write a differential equation for the height h as a function of time. b) Calculate the time it takes to empty the tank. c) Show that when $h_0 \ll L$ the emptying time becomes independent of L. Explain this result physically.

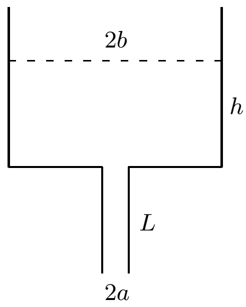

Water tank with a pipe.

18.18 Show that for draining of a cistern (section 18.8), one obtains the following equation for the Reynolds number

$$\mathsf{Re}^2 + 64k\mathsf{Re}f(\mathsf{Re}) = \mathsf{Re}_0^2 \tag{18-72}$$

where $k = L/2a$, $\mathsf{Re}_0 = 2aU_0/\nu$ and $U_0 = \sqrt{2g_0h}$. Show that the corresponding laminar equation is

$$2\mathsf{Re}^2 + 64k\mathsf{Re} = \mathsf{Re}_0^2 \tag{18-73}$$

Explain the differences between these two equations.

18.19 Show that the coefficients of the general solution to circulating flow may be written as

$$A = \frac{\Omega_b b^2 - \Omega_a a^2}{b^2 - a^2} \tag{18-74}$$

$$B = \frac{a^2 b^2(\Omega_a - \Omega_b)}{b^2 - a^2} \tag{18-75}$$

where Ω_a and Ω_b are the angular velocities of the inner and outer cylinders.

18.20 Calculate the total volume of fluid carried along between the cylinders (per unit of axial length and per unit of time) in Couette flow.

18.21 Calculate the total kinetic energy of the fluid in a Couette flow apparatus.

18.22 A semipermeable circular cylindrical pipe carrying water under pressure leaks water into the surrounding water-filled container at a constant rate through its surface. Determine the steady state, maximally symmetric form of the radial flow pattern outside the pipe.

18.23 [**Couette viscometer:**] Consider a torsion-wire Couette viscometer with radii a and $b = a + d$ ($d \ll a$), and axial length $L \gg d$. Let the torque exerted by the torsion wire (from which the inner cylinder hangs) be $-\tau\phi$ where ϕ is the torsion angle. Assume that the inner cylinder has total mass M and is made from very thin shell of homogeneous material. Let the cylinder perform damped torsion oscillations in the presence of the fluid. a) Show that the equation of motion for the torsion angle becomes (for $d \ll a$)

$$Ma^2 \frac{d^2\phi}{dt^2} = -\tau\phi - 2\pi\eta a^3 \frac{L}{d}\frac{d\phi}{dt} \tag{18-76}$$

under the assumption that the fluid flow may be considered quasi-steady at all times. b) Determine the deflection angle for steady rotation. c) Find the condition for critical damping of the oscillations.

18.24 A Couette flow apparatus which is open on the top is placed vertically in gravity g_0. Find the shape of the open fluid surface between the cylinder walls.

18.25 The drive shaft in a truck has a diameter of 15 cm and a bearing of length 10 cm with 1 mm of lubricant of viscosity $\eta = 0.01$ Pa s. a) Calculate the volume discharge in the bearing when the shaft rotates 10 revolutions per second. b) Calculate the rate of heat production.

∗ **18.26** Show that the dissipated power in a stretch of a circular tube is given by (18-31).

18.27 Show directly that the vorticity field of the spindle vortex (18-67) vanishes everywhere.

